NEUROSCIENCE

Termination of convulsion seizures by destabilizing and perturbing seizure memory engrams

Shirong Lai[1,2]†, Libo Zhang[3,4]†, Xinyu Tu[1]†, Xinyue Ma[1]†, Yujing Song[1], Kexin Cao[3,5], Miaomiao Li[6], Jihong Meng[6], Yiqiang Shi[1], Qing Wu[2], Chen Yang[1], Zifan Lan[1], Chunyue Geoffrey Lau[7], Jie Shi[3]*, Weining Ma[6]*, Shaoyi Li[6]*, Yan-Xue Xue[3,8]*, Zhuo Huang[1,9]*

Epileptogenesis, arising from alterations in synaptic strength, shares mechanistic and phenotypic parallels with memory formation. However, direct evidence supporting the existence of seizure memory remains scarce. Leveraging a conditioned seizure memory (CSM) paradigm, we found that CSM enabled the environmental cue to trigger seizure repetitively, and activating cue-responding engram cells could generate CSM artificially. Moreover, cue exposure initiated an analogous process of memory reconsolidation driven by mammalian target of rapamycin–brain-derived neurotrophic factor signaling. Pharmacological targeting of the mammalian target of rapamycin pathway within a limited time window reduced seizures in animals and interictal epileptiform discharges in patients with refractory seizures. Our findings reveal a causal link between seizure memory engrams and seizures, which leads us to a deeper understanding of epileptogenesis and points to a promising direction for epilepsy treatment.

INTRODUCTION

Temporal lobe epilepsy, one of the most common neurological diseases, arises from long-lasting changes in synaptic strength between neurons. These changes resemble both the mechanistic and phenotypic aspects of hippocampus-dependent memory formation (*1*, *2*). Decades ago, Goddard and Douglas (*3*) put forward the opinion that the engram of epilepsy is analogous to the engram of normal long-term memory. Recently, modeling studies suggested that epilepsy may arise as an abnormal learned response; thus, it could potentially be treated and reversed through unlearning (*4*). The high similarity between memory formation and epileptogenesis is increasingly noticed and highlighted to provide promising avenues for epilepsy research (*1*, *2*). For example, despite seizures occurring spontaneously in most patients with epilepsy, reflex epileptic seizures occur recurrently in response to specific triggers (*5*–*7*). The context dependency in reflex epilepsy phenotypically resembles the associative memory formed in classical conditioning (*8*), which is a robust and straightforward form of learning and memory (*9*–*11*). Furthermore, multiple studies revealed that cellular plasticity mechanisms involved in memory formation/disintegration (long-term potentiation/long-term depression) also play a crucial part in processes inducing/reversing epileptic activity (kindling/low-frequency electrical stimulation) (*3*, *12*–*14*). Regarding neural circuit studies, seizure-induced activities can be consolidated as specific neuronal assemblies, similar to learning and memory functions (*15*, *16*). Although all these parallels suggest a potentially close relationship between them, the existence of a process analogous to memory formation in epileptogenesis has not yet been demonstrated in mammals, direct evidence supporting the existence of classically dynamic memory process of epilepsy remains lacking.

Classical conditioning is a widely used laboratory paradigm to study associative learning and memory (e.g., fear memory), in which unconditioned response could be specifically induced by conditioned stimulus (CS) after being paired with unconditioned stimulus (US) (*17*). Recent advances in experimental technologies have allowed scientists to precisely identify and manipulate engram cells (*18*–*20*). According to the memory engram theory, engram cells are a population of neurons that are activated during learning, have enduring cellular changes as a consequence of learning, and can be reactivated by a part of the original stimuli delivered during learning, resulting in memory recall (*20*, *21*). However, the seemingly long-lasting memories are actually dynamic: Retrieved memories are transiently destabilized and undergo a following protein synthesis–dependent process called reconsolidation (*22*–*24*). This process is concomitant with engram restabilization (*21*). During the specific time window (usually minutes to hours) of reconsolidation, memories are rendered labile and susceptible to impairment, providing viable opportunities to therapy pathological memories (*24*–*27*). Given the high analogy between epilepsy and memory, we hypothesized that seizure might store in specific memory engrams, and targeting the analogous process of reconsolidation could interrupt seizures.

RESULTS

Development and validation of a conditioned seizure memory paradigm in rodents

First, we predicted that epileptic seizures could be associated with specific cues. To verify this idea, we developed a novel conditioned

[1]State Key Laboratory of Natural and Biomimetic Drugs, Department of Molecular and Cellular Pharmacology, School of Pharmaceutical Sciences, Peking University Health Science Center, Beijing 100191, China. [2]School of Health Management, Xihua University, Chengdu 610039, China. [3]National Institute on Drug Dependence and Beijing Key Laboratory of Drug Dependence, Peking University, Beijing 100191, China. [4]Shenzhen Public Service Platform for Clinical Application of Medical Imaging, Shenzhen Key Laboratory for Drug Addiction and Medication Safety, Department of Ultrasound, Peking University Shenzhen Hospital, Shenzhen-PKU-HKUST Medical Center, Shenzhen 518036, China. [5]Department of Pharmacology, School of Basic Medical Sciences, Peking University, Beijing 100191, China. [6]Department of Neurosurgery, Shengjing Hospital of China Medical University, Shenyang 110022, China. [7]Department of Neuroscience, City University of Hong Kong, Hong Kong SAR, China. [8]Chinese Institute for Brain Research, Beijing 102206, China. [9]IDG/McGovern Institute for Brain Research, Peking University, Beijing 100871, China.
*Corresponding author. Email: shijie@bjmu.edu.cn (J.S.); maweining1985@163.com (W.M.); lishaoyi2097@163.com (S. Li); yanxuexue@bjmu.edu.cn (Y.-X.X.); huangz@hsc.pku.edu.cn (Z.H.)
†These authors contributed equally to this work.

seizure memory (CSM) paradigm to test whether the seizure onset could be paired with a specific sensory cue. In this paradigm, we adopted the commonly used chemical-induced seizures (CISs) as the US and olfactory/auditory cues as the CS.

During the training session, mice were intraperitoneally injected with kainic acid (KA; 20 mg/kg) to induce CIS. Throughout the training session, the mice were exposed to an odor (lemon odor) for CIS + odor pairing group (*28*), while the control group received CIS or odor alone (Fig. 1, A and B, and see Materials and Methods). Two weeks later, in test session, the mice were exposed to the CIS-paired odor or a novel odor (osmanthus odor) for 15 min to test whether epileptic seizures could be induced by the CIS-paired/CIS-unpaired odor (Fig. 1B). The onsets of electrographic seizure were examined using video electroencephalogram (EEG) recordings, and the convulsion seizure severity was assessed according to Racine's classification (*29*) and epileptiform discharges (Fig. 1C).

We found that during the cue-induced seizure test, the mice trained with CIS + lemon odor pairing had remarkably more electrographic or convulsion seizures than the mice trained with the lemon odor alone (no seizures group) or CIS alone, suggesting that the lemon odor per se does not induce seizures and odor-conditioned seizure memories were created and retrieved in our seizure conditioning paradigm. In addition, upon exposure to a novel osmanthus odor (CIS + odor, novel odor group), the mice did not show increased onset of seizure, suggesting that odor-conditioned seizure memories created in our seizure conditioning paradigm can be retrieved specifically by the CIS-paired odor (Fig. 1, D and E). Consistently, the CIS + odor pairing group mice had a significantly longer total seizure duration during the test session (Fig. 1, D and F). We also detected a few seizures during the test session in the CIS alone and novel odor group mice, which may be due to spontaneous seizures after KA-induced status epilepticus (*30*–*32*).

If the conditioned seizure memories are stored stably after the formation, then they could be retrieved repetitively. To test this, we designed an experimental protocol for the seizure conditioning paradigm with three test sessions: 2 weeks after CIS + odor pairing, mice were tested with reexposure to the CIS-paired odor three times at 1-week intervals (Fig. 1G). We found that exposure to the paired odor elicited a robust increase in times of seizures and a longer total seizure duration during the three consecutive CSM tests (Fig. 1, H and I, and fig. S1). Thus, cue-induced CSM is stable and long-lasting.

Next, we wondered whether alternative type of cue could also be specifically associated with CIS. We replaced odors with sounds as the conditioned cue in the seizure conditioning paradigm described above to investigate whether sound-conditioned seizure memories can be established in mice. As expected, during the CSM test, the mice trained with CIS + paired sound exhibited significantly more severity of seizures than the group trained with the sound alone or tested with exposure to a novel sound, reflected in both number of seizures and total seizure durations (fig. S2). Moreover, we extended the validation of the CSM paradigm to include additional scenarios. First, we assessed its effectiveness in female mice (fig. S3, A and B), demonstrating that CSM could be established across sexes. Second, we applied the paradigm to an electrical kindling seizure model (fig. S3, C and D), where it consistently yielded results in line with our previous findings. Last, we conducted experiments in rats (fig. S3, E to G), further confirming the ability of the CSM paradigm to form conditioned seizure memories across different species and seizure models.

Creation of an artificial CSM by activating cue-responding engram cells

Engram cells are a subset of neurons that are activated during learning and can be reactivated by a part of the original stimuli delivered during learning, resulting in memory recall (*20*, *21*). Accordingly, some pioneering studies have found that associative fear memories can be created by pairing artificial activation of context-responding engram cells with fear (*33*, *34*). To further explore the association between cues and CIS in our seizure conditioning paradigm, we asked whether odor-conditioned seizure memories can also be created in hippocampal dentate gyrus (DG) neurons by pairing chemogenetic activation of odor-responding engram cells with CIS. The DG has been functionally associated with olfactory circuits (*35*) and memory formation (*36*). To confirm that a subpopulation of DG neurons is responsive to the olfactory stimuli, we first detected transient c-fos expression by immunofluorescence staining of the hippocampus 1.5 hours after exposure to an odor (fig. S4). Consistent with previous investigations (*37*), there were significantly more c-fos$^+$ cells in the DG of mice exposed to the lemon odor than to no specific odor, supporting activation of DG neurons upon exposure of mice to the olfactory stimulus.

To artificially activate odor-responding engram cells in the DG upon pairing with CIS, we first combined a neural activity–dependent labeling system with chemogenetics (*38*, *39*). We bilaterally infused the DG with a viral cocktail, which is a combination of adeno-associated viruses for the enhanced synaptic activity-responsive element (E-SARE)–driven tamoxifen-dependent estrogen receptor-dependent Cre-recombinase (ERCreER) (AAV9-pFBAAV-E-SARE-ERCreER-PEST) and Cre-inducible hM3DGq-mCherry protein (AAV8-EF1a-DIO-hM3DGq-mCherry). Three weeks later, mice were exposed to the odor stimulus for 15 min immediately after 4-hydroxytamoxifen (4-OHT) administration. Under the control of the E-SARE promotor and the presence of 4-OHT, the activated DG neurons responsive to the odor stimulus were captured with permanent hM3DGq-mCherry expression (Fig. 2, A to C).

To investigate the specificity of the neural activity–dependent labeling system, we reactivated the DG neurons with an additional stimulus with the same odor (lemon), a novel odor (osmanthus), or no odor 1 week after the neural activity–dependent labeling (Fig. 2D). The proportion of double-labeled DG neurons (mCherry$^+$/c-fos$^+$) among all mCherry$^+$ neurons was profoundly higher in mice exposed to the same odor than other two groups (Fig. 2, E and F). This suggests that the odor-responding engram cells in DG can specifically encode an odor, and these engram cells can be accurately reactivated by the same odor.

With the odor-responding engram cells in the DG specifically captured and prepared for manipulation, we continued pairing artificial activation of odor-responding engram cells with CIS to investigate whether odor-conditioned seizure memories can be created. Odor-responding engram cells in the DG were labeled and permanently expressed hM3DG(q) in mice 1 week before the training session. During the training session, mice were injected with clozapine *N*-oxide (CNO) 30 min before KA to ensure that the captured odor-responding engram cells were activated during CIS (CIS + artificial odor, i.e., chemogenetic activation of odor engram cells pairing). As controls, mice were trained with CIS alone or chemogenetic activation of odor engram cells alone (i.e., without pairing). Two weeks later, mice were exposed to the same odor again to test whether epileptic seizures could be successfully induced (Fig. 2G). Upon exposure to

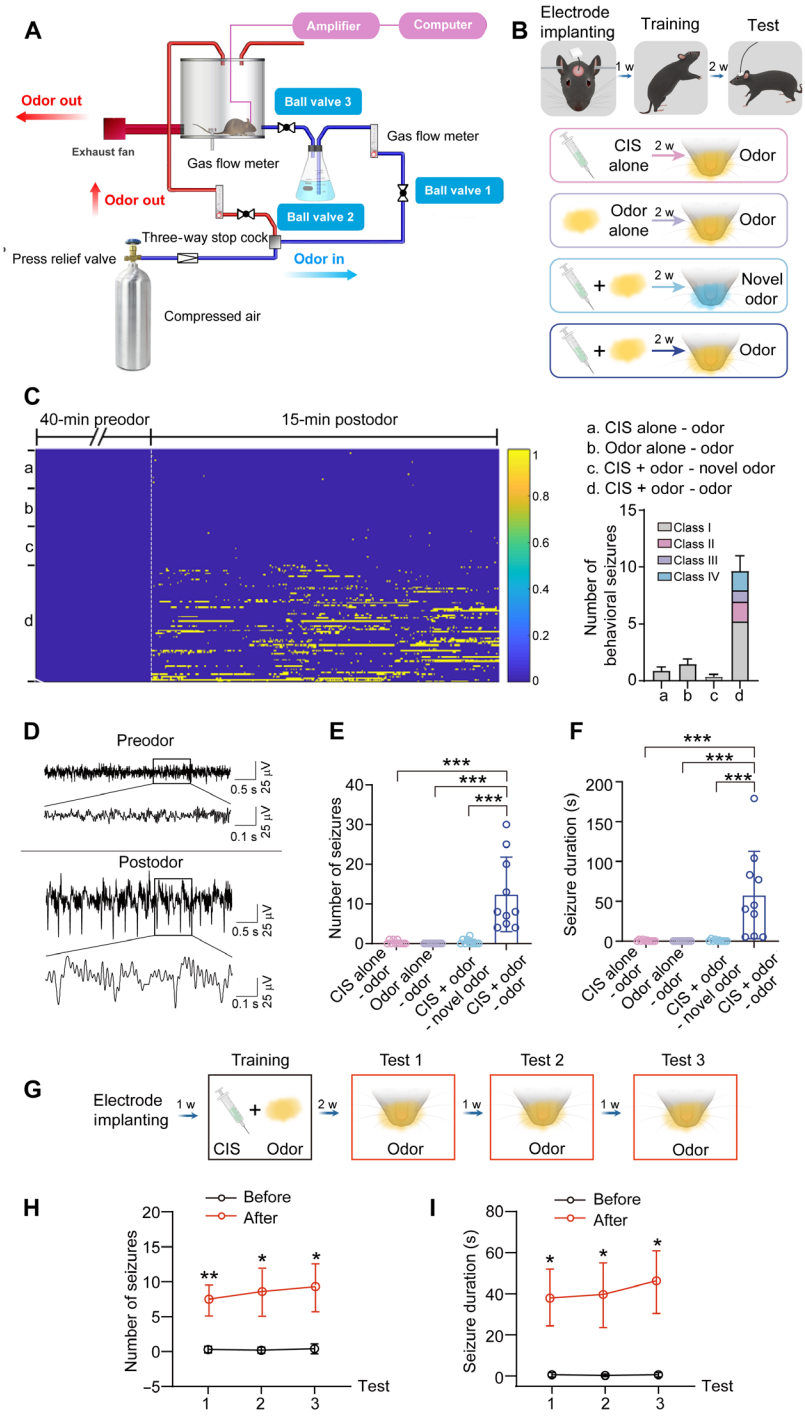

Fig. 1. Development and validation of a CSM paradigm in mice. (**A**) Schematic illustration of the video EEG recording setup and the odor delivery system. (**B**) The experimental procedure for seizure conditioning. After electrode implantation, mice underwent simultaneously training with CIS alone (pink) or odor alone (light purple) or CIS paired with a specific odor (CIS + odor; blue). In the test session conducted 2 weeks (2 w) later, mice were exposed to the CIS-paired odor, except that the mice were tested with a novel odor (light blue). (**C**) Example timelines (left) and statistics (right; averages with error bars indicating SEM) indicating the seizure onsets under pre- and postodor exposure conditions in (B), one mouse per row. The width of the vertical line represents the duration of the seizure onset. (**D**) Typical EEG traces recorded under pre- and postodor exposure conditions in test sessions [red in (B)] showing the spike wave discharges associated with seizure onsets. (**E** and **F**) Graphs depicting the number of seizures (E) and seizure duration (F) during the 15-min test session after applying the odor test illustrated in (B) (each group, $n = 10$). Dots represent individual animals; data are presented as means ± SD. (**G**) Timeline of experimental protocol for seizure conditioning. Two weeks after the training session under CIS + odor pairing condition, mice with electrodes previously implanted were tested repeatedly with the CIS-paired odor (three tests, at 1-week intervals). (**H**) Graphs depicting the number of seizures in (G); data are presented as means ± SEM. (**I**) Graphs depicting seizure duration in (G) recorded from mice before and after odor exposure during the three test sessions ($n = 10$). Data are presented as means ± SEM; $^{*}P < 0.05$, $^{**}P < 0.01$, and $^{***}P < 0.001$.

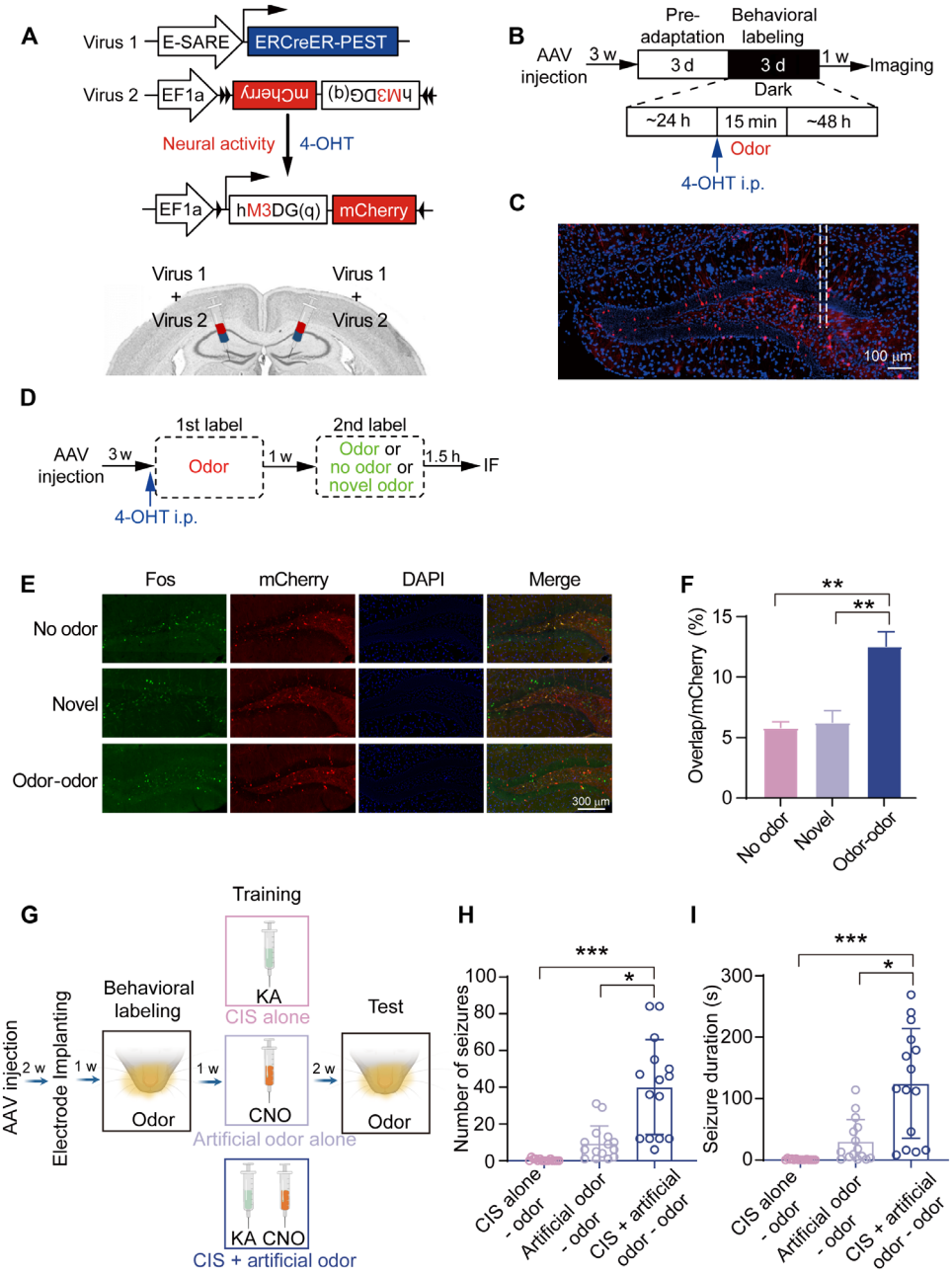

Fig. 2. Pairing chemogenetic activation of odor-responding engram cells in the DG with CIS created artificial CSM. (**A**) Experimental scheme illustrating the neural activity–dependent labeling of engram cells in the hippocampal DG area. A subpopulation of DG neurons responding to the olfactory stimulus expresses ERCreER under the control of the E-SARE promotor. In the presence of 4-OHT, these neurons permanently express mCherry and hM3DG(q), enabling subsequent imaging and manipulation, respectively. (**B**) Timeline depicting the neural activity–dependent behavioral labeling protocol. i.p., intraperitoneally. (**C**) Representative microscopic image of DG showing viral injection site and with odor-responding engram cells labeled (red). Blue fluorescence is 4′,6-diamidino-2-phenylindole (DAPI). (**D**) Timeline for the specificity test of the activity-dependent labeling system. IF, immunofluorescence. (**E**) Representative microscopic images from mice in (D) showing DG neurons labeled with mCherry (red) and/or c-fos (green). DG neurons activated during lemon-lemon test in (D) expressed both (yellow; merged). (**F**) Quantifications of the proportion (%) of c-fos$^+$/mCherry$^+$ overlapping neurons among all mCherry$^+$ DG neurons [each group, $n = 4$ mice; one-way analysis of variance (ANOVA) followed by Dunnett's multiple comparisons]. Data are presented as means ± SEM. (**G**) The procedure for seizure conditioning with the chemogenetic activation of odor-responding engram cells in DG. (**H** and **I**) Graphs depicting the number of seizures (H) and seizure duration (I) (unequal variance, Kruskal-Wallis test followed by Dunn's multiple comparisons) recorded during the test session from mice under the three conditions in (G) (each group, $n = 15$ mice). Dots represent individual animals; data are presented as means ± SD; ***$P < 0.001$, **$P < 0.01$, and *$P < 0.05$.

the lemon odor, the mice trained with CIS + chemogenetic activation of odor engram cells pairing displayed significantly more severity of seizures and longer total seizure duration than the CIS alone or the chemogenetic activation of odor engram cell alone group mice (Fig. 2, H and I).

In parallel with the chemogenetic activation experiments, we conducted a chemogenetic inhibition experiment following a similar procedure. Mice underwent bilateral infusion of the DG with a viral cocktail containing AAV9-pFBAAV-E-SARE-ERCreER-PEST and AAV8-EF1a-DIO-hM4DGi-mCherry. Two weeks later, 4-OHT was administered to label odors, inducing the expression of hM4DGi-mCherry. During the training session, mice in the CIS + artificial no odor group and the CIS + odor group were injected with CNO or saline before odor-paired KA-induced seizure training, respectively. Consistent with our previous experiment, upon exposure to the lemon odor in the test session, less number of seizures and shorter total seizure duration was observed in mice received CNO than saline, which indicates that the chemogenetic inhibition of odor-responsive engrams by CNO (i.e., artificial no odor) disrupted the formation of these odor-conditioned seizure memories (fig. S5).

Here, we successfully established a model in which artificial targeting odor-responding engram cells paired with CIS could influence odor-conditioned seizure memories. We also confirmed that these odor-conditioned seizure memories could be specifically retrieved by the odor involved in the formation of engram cells.

Seizure memory retrieval triggers a protein synthesis–dependent memory reconsolidation

For the process of memory reconsolidation, protein synthesis is an underlying mechanism that is necessary for the maintenance of long-term memories (*22*, *23*, *40*, *41*) and requires multiple signaling pathways, including brain-derived neurotrophic factor (BDNF) (*42*), early growth response factor 1 (EGR1) (*43*), mammalian target of rapamycin (mTOR) (*44*, *45*), and extracellular signal–regulated kinase (ERK) (*46*, *47*). To deeply understand the retrieval and reconsolidation process of the CSM, we investigated the dynamic changes of these memory-related proteins/pathways in the hippocampus after memory retrieval in our CSM model. Mice were first trained with CIS + odor pairing. Two weeks later, odor-conditioned seizure memories were retrieved by exposure to the lemon odor, and mice were decapitated at 15 min, 1 hour, 2 hours, or 9 hours after odor exposure (Fig. 3A). As controls, mice were decapitated before exposure to the lemon odor. The memory-related proteins expressed in the hippocampus of these nonretrieval group mice were measured and used as the baseline expression levels for comparisons.

We found that after the retrieval of odor-conditioned seizure memories, the expression of phosphorylated ERK (pERK) and phosphorylated mTOR (pmTOR) were significantly increased at 1 hour (Fig. 3, B to E), while the peak level of BDNF was at 2 hours (Fig. 3, F and G). Moreover, the expression of all these memory-related proteins returned to the baseline levels at 9 hours after retrieval of odor-conditioned seizure memories. No significant changes in the expression level of EGR1, total ERK, or total mTOR were observed after retrieval of odor-conditioned seizure memories compared to the baseline level (Fig. 3, C, E, and H). These results suggest that exposure to seizure memory cues triggers time-dependent dynamic changes in several memory-related signaling pathways, supporting that the same pathways previously demonstrated in physiological memories (*48*–*50*) are also engaged in the odor-conditioned seizure memories.

To confirm whether the protein synthesis was essential for reconsolidation of CSM, we used anisomycin to inhibit protein synthesis (*22*) and thus impair the memory reconsolidation of CSM (Fig. 3I). We applied systemic injection of anisomycin to mice immediately after exposure to the odor cue (test 1 in Fig. 3I) to find out whether odor-conditioned seizure memories could be abolished in the following retrieval sessions (test 2 in Fig. 3I). One week later, upon re-exposure to the lemon odor (test 2 in Fig. 3I), the mice received anisomycin at 5 min (within the reconsolidation time window) after the retrieval of odor-conditioned seizure memories had markedly fewer numbers of seizures and shorter total seizure duration than the control mice received vehicle (Fig. 3J). In contrast, the mice received anisomycin at 9 hours (outside the reconsolidation time window) after the retrieval of odor-conditioned seizure memories had similar seizure times and durations compared to vehicle (Fig. 3K). Thus, these data suggest that after retrieval of seizure memory, inhibiting the protein synthesis process within the reconsolidation time window impaired the retrieval of CSM, which may provide a novel therapeutic strategy for seizure treatment.

Blockade of mTOR pathway within the reconsolidation time window terminates seizure onset in mice

Targeting the proteins or pathways involved in the memory reconsolidation process within the limited time window to disrupt the reconsolidation process has been proposed as a potential strategy to impair problematic memories (*27*), including fear conditioning memory (*51*, *52*), posttraumatic stress disorder (*53*), and drug addiction (*54*, *55*). Since mTOR pathway, ERK pathway, and BDNF are indispensable for reconsolidation of CSM, we explored whether blockade of these pathways during the reconsolidation time window can attenuate CSM (Fig. 4A).

We used rapamycin and propranolol as the inhibitors of mTOR or ERK (*56*) pathways, respectively. We found that the mice that received immediate administration of either rapamycin or propranolol after retrieval of seizure memories had significantly fewer seizures and shorter total seizure duration than control mice that received vehicle 1 week later (Fig. 4, B and F), while delayed administration of rapamycin or propranolol at 9 hours after the first retrieval of odor-conditioned seizure memories had no effect on the subsequent seizure onset (Fig. 4, D and H). Consistently, significantly decreased levels of BDNF, pERK, and pmTOR in hippocampal were detected in mice that received immediate drug administration (Fig. 4, C and G), while delayed administration of rapamycin or propranolol at 9 hours did not change the expression levels of these proteins (Fig. 4, E and I). These findings suggest that immediate intervention with rapamycin or propranolol to disrupt the mTOR or ERK pathways during the reconsolidation process can impair the postreconsolidation retrieval of odor-conditioned seizure memories. We also confirmed that targeting BDNF during the memory reconsolidation process could impair postreconsolidation retrieval of odor-conditioned seizure memories (fig. S6). Together, these findings demonstrate that it was an effective strategy to attenuate CSM by blocking mTOR-BDNF within the limited time window of reconsolidation.

Targeting mTOR pathway within the reconsolidation time window decreases interictal epileptiform discharges in patients with refractory seizure

On the basis of compelling results from animal models, we conducted a randomized pilot study to assess the effects of targeting memory

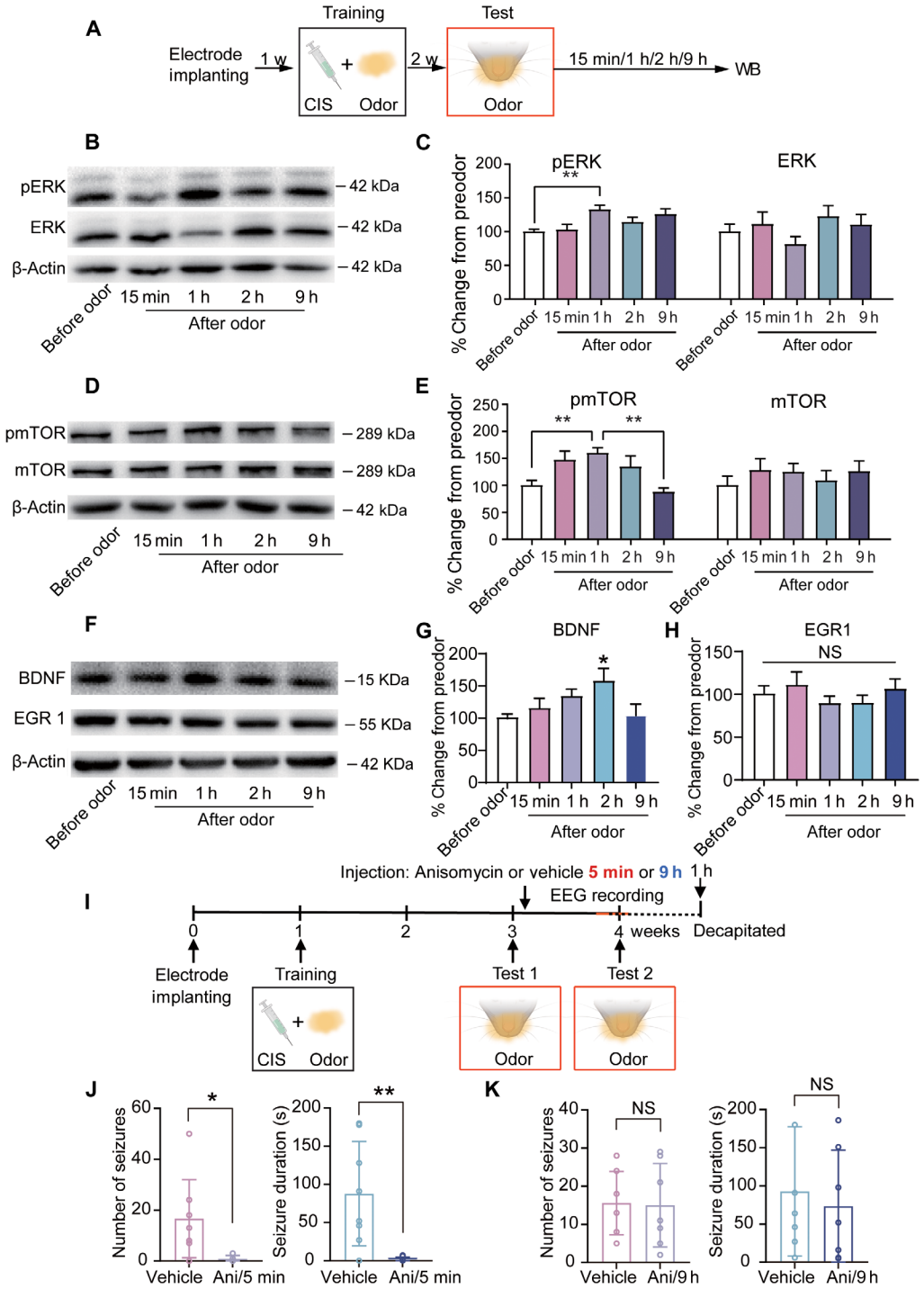

Fig. 3. Retrieval of CSM led to a protein synthesis–dependent reconsolidation process in the hippocampus. (**A**) Timeline for protein detection after retrieval of CSM from the seizure conditioning paradigm. Mice were decapitated before (control) or at 15 min, 1 hour, 2 hours, or 9 hours after the retrieval session. (**B** to **H**) Representative Western blot (WB) images and quantification indicating the expression levels of pERK and total ERK (C), pmTOR and mTOR (E), BDNF (G), and EGR 1 (H), in the hippocampus of mice decapitated before odor exposure (control) and at the indicated time points after odor exposure [each group, $n = 8$ mice; two-way ANOVA followed by Tukey's post hoc test in (C) and (E); one-way ANOVA followed by Dunnett's multiple comparisons to preodor in (G and H)]; β-actin served as a loading control. Error bars represent the SEM; $^*P < 0.05$. NS, not significant. (**I**) Timeline of the experiment. Anisomycin (Ani) or vehicle was administrated immediately (at 5 min) or delayed for 9 hours after the first retrieval of CSM at week 3 (test 1). Mice were tested with reexposure to the CIS-paired odor at week 4 (test 2). (**J** and **K**) Graphs depicting number of seizures and seizure duration recorded during the test session from mice with the treatment of immediate (J) or delayed (K) anisomycin or vehicle after the first retrieval [immediate vehicle or anisomycin, $n = 8$ mice, each; two-tailed Welch's t tests in (J); two-tailed unpaired t tests in (K)]. Dots represent individual animals; data are presented as means ± SD. $^*P < 0.05$ and $^{**}P < 0.01$.

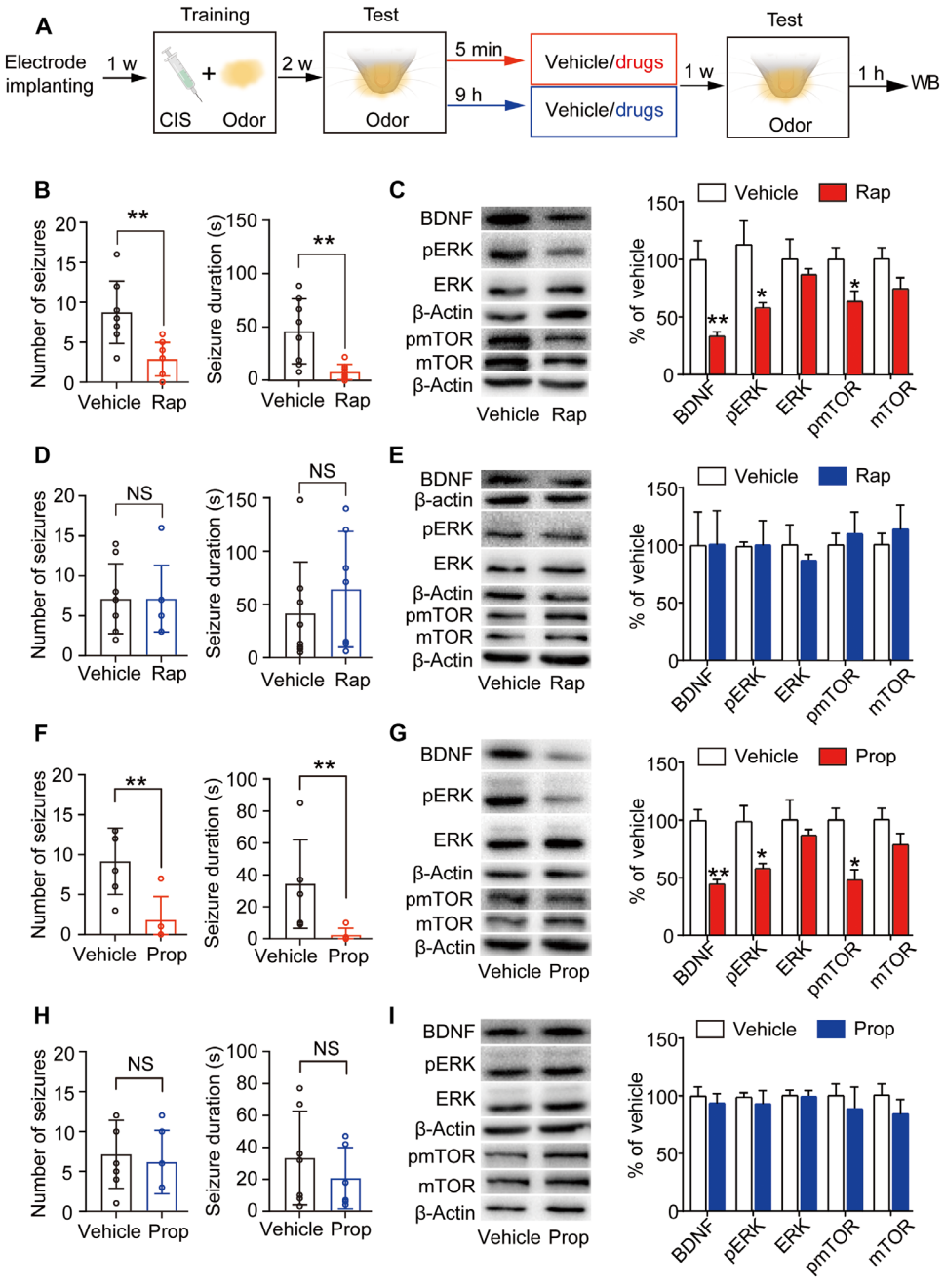

Fig. 4. Pharmacological intervention targeting mTOR or ERK pathway within the reconsolidation time window impaired the persistent of CSM. (**A**) Timeline of the pharmacological intervention experiments. (**B** and **D**) Graphs depicting the number of seizures and seizure duration recorded during the test session from mice with the treatment of immediate (B) or delayed (D) rapamycin (Rap) or vehicle after the first retrieval (immediate vehicle, $n = 8$; immediate rapamycin, $n = 8$; delayed vehicle, $n = 8$; delayed rapamycin, $n = 7$). (**C** and **E**) Representative Western blot images and quantification indicating the expression levels of BDNF, pERK1/2, total ERK1/2, pmTOR, and total mTOR in the hippocampus of mice decapitated 1 hour after the test session with the treatment of immediate (C) or delayed (E) rapamycin or vehicle after the first retrieval (each group, $n = 6$). (**F** and **H**) Graphs depicting the number of seizures and seizure duration with the treatment of immediate (F) or delayed (H) propranolol (Prop) or vehicle after the first retrieval (immediate vehicle, $n = 6$; immediate propranolol, $n = 5$; delayed vehicle, $n = 7$; delayed propranolol, $n = 6$). (**G** and **I**) Representative Western blot images and quantification indicating the expression levels of BDNF, pERK1/2, total ERK1/2, pmTOR, and total mTOR 1 hour after the test session with the treatment of immediate (G) or delayed (I) propranolol or vehicle after the first retrieval (each group, $n = 6$). β-Actin served as a loading control. Data are presented as means ± SD in (B), (D), (F), and (H); data are presented as means ± SEM in (C), (E), (G), and (I). Two-tailed unpaired *t* tests in [(B), left], (C), (E), [(F), left], (G), [(H), left], and (I); two-tailed Welch's *t* tests in [(B), right], [(F), right], and [(H), right]. $^*P < 0.05$ and $^{**}P < 0.01$.

reconsolidation therapy on the onset of epilepsy in patients with refractory seizures. We evaluated the impact of everolimus, an mTOR inhibitor, on refractory epilepsy at different administration times. Specifically, nine refractory epilepsy patients were enrolled in this study and randomly assigned to three groups: 1-hour treatment group within the reconsolidation time window, 8-hour delayed treatment group, and the negative control group. They orally received a single dose of either everolimus or placebo (vitamin C) 1 hour or 8 hours after an epileptic seizure.

EEG was monitored through the predrug period (baseline) to the postdrug period for each patient. Interictal epileptiform discharges (IEDs) recorded in EEG are generally considered to reflect the hyperexcitability of neuronal cells causing the seizure onset, and the reduction of IEDs may represent a beneficial effect of a drug on seizure recurrence (*57*, *58*). Therefore, we compared the frequency of IEDs before and after drug administration. We found that 1-hour everolimus administration significantly decreased IED frequency in all three subjects in the treatment group (Fig. 5, A and D). However, the frequency of IEDs did not change in the 8-hour delayed everolimus treatment group (Fig. 5, B and E) or the placebo control group (Fig. 5, C and F). The data elucidate the effect of everolimus on decreasing IEDs in patients with refractory epilepsy when administered within the reconsolidation time window after epileptic seizure events.

DISCUSSION

Here, we developed a novel CSM paradigm, in which seizures and specific cues were paired. The CSM could be reliably retrieved, demonstrating a robust association. We also found that activation of cue-responding engram cells in DG could create artificial CSM. After seizure memory retrieval, a protein synthesis–dependent reconsolidation process involving BDNF, mTOR, and ERK pathways was observed. Our data show prominent pharmacological intervention effects on disrupting CSM when applied during memory reconsolidation in both rodents and humans. Together, our findings revealed an analogous process between memory and seizure and supplied direct evidence on the insight from physiological memory to understand pathological epilepsy and seizure memory–targeting strategy for the treatment of refractory seizures.

Reflex seizures are specific seizure types triggered by various types of stimuli (*7*), such as sounds (*59*), flickering lights (*60*), a special odor

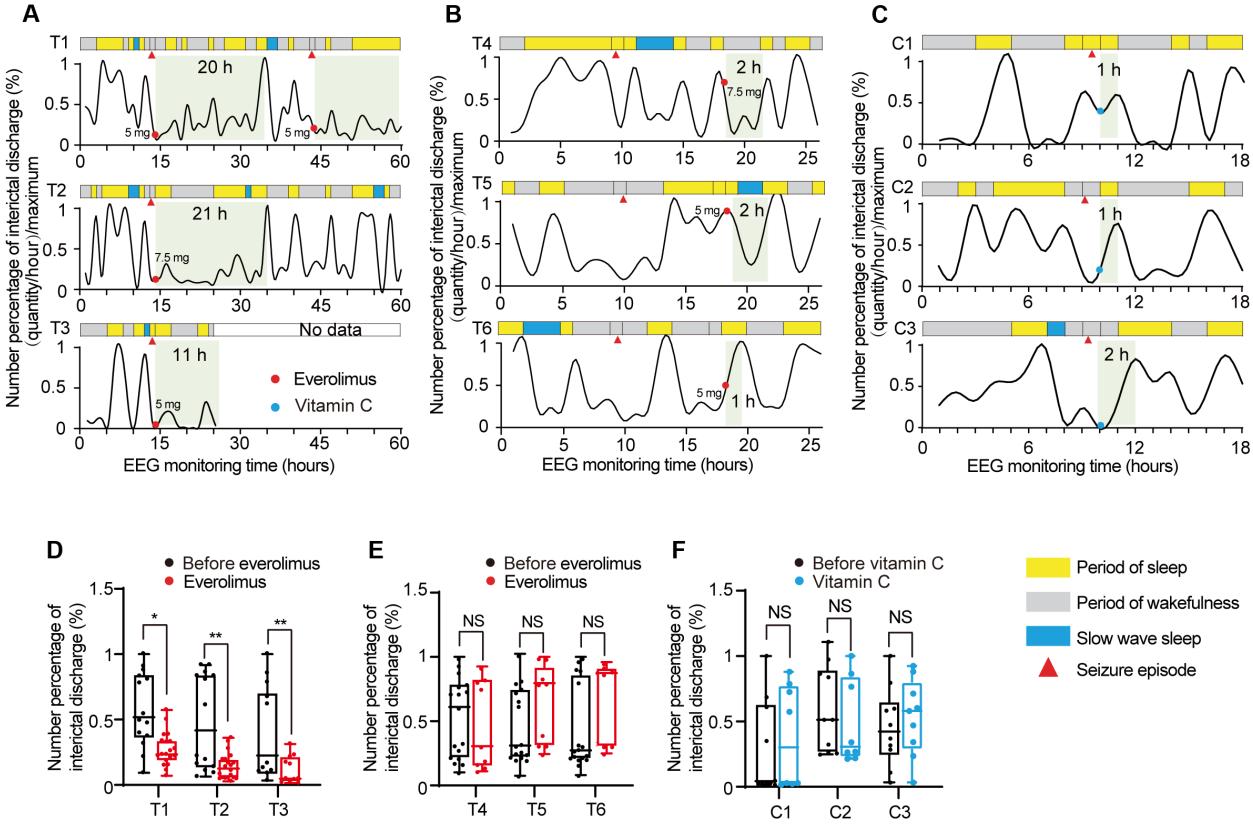

Fig. 5. Targeting mTOR pathway within the reconsolidation time window decreases IEDs in patients with refractory seizure. (**A** to **C**) Temporal profile of epileptiform paroxysmal activities represented by IEDs. The IEDs were observed from 9 to 14 hours preceding the seizure event until 9 to 46 hours after the seizure event, normalized to the maximum discharge number of each patient. The administration of drug or placebo after a seizure event is marked as a red or blue dot in the diagram. The green shadow represents recovery period of IED frequency to basal level. The IEDs were observed from 14 hours preceding the seizure event until 46 hours after the seizure event in the 1-hour everolimus treatment group (T1 to T3) (A), from 9 hours preceding the seizure event until 16 hours after the seizure event in the 8-hour delayed everolimus treatment group (T4 to T6) (B), and from 9 hours preceding the seizure event until 9 hours after the seizure event in the negative control (vitamin C treatment) group (C1 to C3) (C). (**D** to **F**) Comparison of the percentage change in IEDs before and after administration in 1-hour everolimus treatment group (T1 to T3) (D), the 8-hour delayed everolimus treatment group (T4 to T6) (E), and the negative control group (C1 to C3) (F). Data are presented as individual values of each hour and line at median; [(D) and (E)] Wilcoxon rank sum test; $*P < 0.05$ and $**P < 0.01$.

(*61*), or thinking (*62*), but the exact mechanism underlying reflex seizures remains elusive (*63*). Recent evidence reveals that patients with reflex epilepsy exhibit abnormally enhanced functional connectivity (*64*, *65*), pointing to the potential relations between epilepsy and memory. Regarding the activity form of neurons, physiological learning and memory rely on the coordinate firing and wiring of neural ensembles (*21*). Similarly, epileptic seizures involve the repetitive and synchronous activation of subpopulations of neurons (*66*). In addition, plasticity changes ranging from synaptic morphology (*67*) to synaptic functions (*3*, *68*) (e.g., long-term potentiation) have also been observed in epileptic brains, which are recognized biological foundations of learning and memory. Our study demonstrated the existence of memory-like processes in epilepsy, which not only provided a novel paradigm for delineating the seizure memory but also revealed a causal link between seizure memory trace and seizure onset.

Protein synthesis is necessary during memory reconsolidation, involving multiple signaling pathways such as BDNF (*42*), mTOR (*44*, *45*), and ERK (*46*, *47*). Our study consistently demonstrated that targeting any of these pathways within specific time window leads to impaired memory reconsolidation of seizure memory. In recent years, interventions based on memory reconsolidation theory have been widely applied in various pathological memory disorders, including fear conditioning memory (*51*, *52*), posttraumatic stress disorder (*53*), hyperalgesia (*69*), and drug addiction (*54*, *55*).

Recognizing the commonalities between memory processes and epilepsy, there has been a recent proposal to apply therapies for memory disorders to the treatment of epileptic patients (*2*). However, the effectiveness of applying the reconsolidation theory to epilepsy treatment remains unclear. In our study, disrupting seizure memory reconsolidation process by a single-dose administration in the critical time window put forward a potential epilepsy treatment strategy. However, it is still necessary to investigate the long-lasting effect of disrupting seizure memory reconsolidation and to assess the potential risks associated with using an mTOR inhibitor to target memory reconsolidation in clinic setting, such as disrupting memories unrelated to seizures.

Nevertheless, memory reconsolidation targeting strategy still offers several advantages over traditional antiepilepsy drugs (AEDs). As for therapeutic theories, traditional AEDs inhibit hyperexcitation networks to alleviate seizure symptoms, leaving one-third of patients failing to respond (*70*–*72*); while, in this study, drugs were applied to "dissociate" the abnormal memory formed in epilepsy and work efficiently. Furthermore, the single-dose administration during a critical time window in our study differs notably from long-term regular administration of traditional AEDs, which may largely avoid adverse effects related to long-term administration (*73*) and alleviate the physical and financial burden of the treatment.

In summary, our study revealed epileptic seizures as a kind of pathological memory process that shares similar characteristics with physiological memory, which not only can be associated with conditioned cues to form the memory engrams but also can be effectively intervened during the reconsolidation time window. This conceptual framework can help us to better understand and treat seizure from the perceptive of aberrant learning and memory.

MATERIALS AND METHODS

Animals

Male adult Sprague-Dawley rats (150 to 200 g, 6 to 8 weeks), C57BL/6 mice (18 to 20 g, 6 to 8 weeks), and female adult C57BL/6 mice (15 to 18 g, 6 to 8 weeks) were purchased from Charles River Laboratories (Beijing). All animals were housed under a 12-hour light/dark cycle with food and water available ad libitum. All animals were handled in strict accordance with the "Guide for the Care and Use of Laboratory Animals" and the "Principles for the Utilization and Care of Vertebrate Animals," and all animal work was approved by the Institutional Animal Care and Use Committee at Peking University. Each effort was made to minimize animal suffering and the number of animals used. The experiments were blind to viral or drug treatment conditions during behavioral testing.

Stereotaxic surgery

Animals (rats and mice of 6 to 8 weeks) were deeply anesthetized by intraperitoneal injection of sodium pentobarbital (SP) (5 mg/kg). Supplementary doses of less than one-third of the original dose were added when necessary to maintain anesthesia. A pinch test was done on the hind paw of the rat to check the depth of anesthesia. The head of the animal was fixed to the stereotaxic apparatus (RWD Ltd., China) with ear bars. Then, the skull was exposed.

For implantation of microwire electrode arrays, coordinates of regions of interest were determined according to the atlas of rat or mice brain coordinates as follows: rat: anterior/posterior (A/P), −3.5 mm; medial/lateral (M/L), ±2.0 mm; dorsal/ventral (D/V), −2.5 mm; mice: A/P, −1.5 mm; M/L, ±1.0 mm; D/V, −2.0 mm. These coordinates are based on our previous work (*74*). Four stainless screws were tightened onto the skull without piercing through the dura. Screws acted as anchors for electrodes stabilization, while one of them was used as ground. Small craniotomies were performed at corresponding coordinates. Dura was removed carefully to expose the brain tissue. Microwire electrode arrays (Blackrock Microsystems Ltd., manufactured in China) were lowered into target regions separately with a low insertion speed (1 mm/10 min) and then bounded to the screws using dental cement. Last, all arrays were fixed to the cranium using dental cement. After the surgery, each animal was allowed to recover for 1 week in its individual cage with free access to food and water.

Mice prepared for intraperitoneal drug injection were also implanted with guide cannulae (23 gauge; Plastics One) in bilateral hippocampal DG before electrode implantation during stereotaxic surgery. To keep away from the microwire electrode arrays, guide cannulae were implanted according to a constant angle with 20° inclined vertically. The coordinates of mice were A/P of −2.2 mm, M/L of ±2.8 mm, and D/V of −1.8 mm. The cannulae were anchored to the skull with the holder of the stereotaxic apparatus. A stainless-steel stylet blocker was inserted into each cannula to keep it patent and prevent infection. Then, microwire electrode arrays were implanted as described above.

For stereotaxic virus injection, the virus was injected through a pulled glass micropipette connected to a Hamilton syringe (Hamilton Company), which was pumped using a syringe pump device (RWD Ltd.). The pipette was slowly lowered to the DG of the hippocampus at the appropriate coordinates: A/P, −2.0 mm; M/L, ±1.3 mm; D/V, −2.1 mm. All mice were injected bilaterally with 500 nl (each side) of a mixture of two viruses (AAV9-pFBAAV-E-SARE-ERCreER-PEST and AAV8-EF1a-DIO–hM3DGq (or hM4DGi)–mCherry; ratio, 3:10) at a rate of 2 nl/s. After the injection, the pipette was held in place for an additional 10 min before being slowly withdrawn. After the removal of the pipette, the skin incision was sutured and treated with antibiotic cream. All mice were allowed to recover for 2 weeks before microwire electrode arrays implantation if electrophysiology recording was included in the following experiments.

Neural activity–dependent labeling

Neural activity–dependent labeling was carried out 3 weeks after the virus injection. To minimize neuronal labeling by background noise, mice were preadapted to the labeling context and intraperitoneal injection of saline for three consecutive days and then kept in a quiet place with constant darkness from about 24 hours before labeling until 2 days after 4-OHT induction. On the labeling day, 4-OHT (Jusheng, Hubei) was dissolved in ethanol at a concentration of 100 mg/ml and then diluted with 9 vol of corn oil (Sigma-Aldrich) in the dark. Mice received an intraperitoneal injection of 0.2 ml of 4-OHT (2 mg per animal) and were immediately exposed to the lemon odor for 15 min. Two days later, the standard 12-hour light/dark cycle was recovered.

Immunofluorescence and cell counting

After deep anesthesia with SP, mice were euthanized by perfusion with 0.1 M phosphate-buffered saline (PBS), followed by 4% paraformaldehyde. Brains were carefully removed and postfixed in 4% paraformaldehyde for 24 hours and subsequently immersed in 30% sucrose in 0.1 M phosphate buffer for 48 hours. Cryostat coronal sections (20 μm) were obtained using a freezing microtome (Leica). The sections were rinsed in 0.1 M PBS (pH 7.4), and incubated in a blocking solution [5% (v/v) bovine serum albumin and 0.4% (v/v) Triton X-100 in PBS] at room temperature for 1 hour, followed by incubation at 4°C for 24 hours in appropriate primary antibodies in blocking solution. Primary antibodies were applied as follows: c-fos (9F6) rabbit monoclonal antibody [Cell Signaling Technology (CST), 2250S; 1:500] and anti-neuronal nuclei antibody, clone A60 (Sigma-Aldrich, MAB377; 1:500). Afterward, sections were washed three times with PBS, then transferred into appropriate secondary antibodies in PBS, and incubated at room temperature for 3.5 hours. Secondary antibodies were used as follows: donkey anti-rabbit immunoglobulin G (H + L) highly cross-adsorbed secondary antibody, Alexa Fluor Plus 488 (Invitrogen, A32790; 1:500) and donkey anti-mouse immunoglobulin G (H + L) highly cross-adsorbed secondary antibody, Alexa Fluor Plus 594 (Invitrogen, A32744; 1:500). After washing three times with PBS, sections were lastly mounted and coverslipped with mounting medium (Solarbio, S2110). Fluorescence images were taken using a microscope (Olympus) with a 20× objective lens to count c-fos$^+$, mCherry$^+$, or overlapped immunoreactive cells in the DG. An investigator blind to treatment counted and averaged the number of immunoreactive cells in DG from three to five coronal slices (spaced at least 60 μm from each other) per mouse using ImageJ. In the specificity test of the activity-dependent labeling system (Fig. 2, D to F), the proportion of overlapped neurons among all mCherry$^+$ neurons in the DG was calculated and averaged for each mouse. For the olfactory stimuli responding experiment (fig. S4), the quantification of c-fos$^+$ cells involved counting their number within the DG granular cell layer.

Antibodies and reagents

Commercial antibodies used were as follows: rabbit anti-BDNF (Abcam, ab108319), rabbit anti-EGR1 (ProteinTech, 55117-1-AP), rabbit anti-pmTOR (Ser^{2448}) (CST, #5536), rabbit anti-mTOR (CST, #2983), mouse anti–β-actin (ZSGB-BIO), rabbit anti–ERK1 + ERK2 (Abcam, ab17942), and mouse anti–Erk1 (pT202/pY204) + Erk2 (pT185/pY187) (Abcam, ab50011). KA, anisomycin, and propranolol were from Sigma-Aldrich. Rapamycin (R-5000) was from LC Laboratories.

Drugs and drug injection procedures

For in vivo chemogenetic activation of hM3DG(q) or hM4DG(i) receptors, CNO (1.5 and 3 mg/kg) dissolved in dimethyl sulfoxide and diluted with saline was intraperitoneally injected at 30 min before and after the training session, respectively. Anisomycin was dissolved in HCl (1 M) and diluted with saline to a concentration of 10 mg/ml (the pH was adjusted to 7.4 with 5 M NaOH). After the induction sessions, mice received anisomycin (75 mg/kg) or an equivalent volume of saline. This amount of anisomycin has been shown to yield >90% protein synthesis inhibition in the brain during the first 2 hours (*75*). Immediately before experimentation, a fresh solution of the drug was made by dissolving rapamycin in a vehicle of 5% ethanol, 4% PEG 400, and 4% Tween 80 in distilled water to a concentration of 1 mg/ml. Mice received rapamycin (40 mg/kg) or an equivalent volume of vehicle after induction sessions. Propranolol was dissolved in saline to a concentration of 2.5 mg/ml. Mice received propranolol (20 mg/kg) or an equivalent volume of saline after induction sessions. As for these drugs, mice were administered by intraperitoneal injection. BDNF antisense oligodeoxynucleotide (ODN) [BDNF antisense ODN (ASO); 5′-TCTTCCCCTTTTAATGGT-3′] or BDNF missense oligodeoxynucleotide [BDNF missense ODN (MSO); 5′-ATACTTTCTGTTCTTGCC-3′] were dissolved in sterile artificial cerebrospinal fluid to a concentration of 2 mM. ASO contained antisense sequences with positive matches only for BDNF mRNA sequences, and no other mammalian coding sequences. Control MSO contained missense sequences, which included the same base composition as the ASO but in a randomized order, and showed no homology with any mammalian sequence in the GenBank database. To protect against nuclease degradation, all of the ODNs (Sangon, Shanghai, China) were phosphorothioated on the three terminal bases at each end and purified by high-performance liquid chromatography. As the ODNs diffused throughout the dorsal hippocampus and only slightly into other areas by 90 min after infusion into the dorsal hippocampus (*76*), they were injected 90 min before the induction sessions. All the ODNs were injected with Hamilton syringes connected to 30 gauge injectors (Plastics One). The infusion volume was 0.4 μl, and the drug was injected bilaterally over 5 min; the injection needle was kept in place for an additional 5 min to allow for drug diffusion.

In vivo EEG recording and data preprocessing

The multichannel recording system was manufactured by Blackrock Microsystems Limited (Salt Lake City, UT, USA). Electrophysiological data were recorded from the implanted microwire electrode arrays. One preamplification headstage was used to record from two electrodes. The analog signals were filtered by a band-pass filter set between 0.3 and 7500 Hz. Then the signals were digitized by the neural signal processor. The local field potentials were recorded at a sampling rate of 1 kHz/s. EEG data were analyzed by EEGLAB tools over MATLAB. The onsets of seizure were confirmed by both EEG and video recordings according to Racine's classification and epileptiform discharges. For EEG recording, epileptiform discharges were recognized by their large amplitudes (≥3 times of background signals), repetitive single, or complex spike waveforms and were confirmed using video recordings.

To remove movement artifacts and other correlated noise, independent component (IC) analysis (EEGLAB toolbox of MATLAB) was applied to all recorded channels first. The IC analysis algorithm was used to isolate sources with different spatial distributions while conserving their temporal information. Decomposed ICs were inspected by both waveforms and weight distribution across recording

channels manually. ICs with slow and large fluctuations temporally correlated to the animal movement were treated as movement artifacts and thus removed from further analysis. Events with large movement artifacts were ruled out from further analysis. After the source identification process, ICs were converted back to the original waveform. By the end of the data preprocessing, two denoised channels were prepared for further analysis.

Chemical-induced seizures

KA was intraperitoneally administered to produce class V seizures as the CIS during the training session. The dose of KA used was 10 mg/kg for rats (6 to 8 weeks) (*77*) and 20 mg/kg for mice (6 to 8 weeks) (*78*, *79*). To assess epilepsy susceptibility, seizures were rated using a modified Racine scale (*80*): (i) immobility followed by facial clonus, (ii) masticatory movements and head nodding, (iii) continuous body tremor or wet-dog shakes; (iv) unilateral or bilateral forelimb clonus; and (v) rearing and falling. Seizures were terminated 1 hour after onset with the use of sodium pentobarbital (SP, 30 mg/kg; Sigma-Aldrich). Control groups were treated with SP only (30 mg/kg).

CSM paradigm

CSM acquisition and testing were performed in a transparent chamber (30 cm by 30 cm by 30 cm, custom-made). The front and top of the chamber were made of clear acrylic, while the other sides were made of opaque white acrylic. Each chamber had an infrared camera at the front to monitor the animal's behavior inside. The paradigm consisted of one training session and one or more test sessions.

Habituation

Mice were handled before the training session to acclimate them to the experimental environment and reduce orienting responses. One week after surgery, mice were handled and habituated to the connection of electrode arrays and wires (3 to 5 days).

Conditioning

On the day of the experiment, mice were placed in a chamber for 15 min to adapt the wire connected to the recording system. In the training session, the CIS was used as the US, and olfactory or auditory cues were used as the CS. For olfactory cues, lemon odor and osmanthus odor were used as the olfactory CS+ (CIS-paired CS) and CS− (CIS-unpaired CS). For auditory cues, sound (2 kHz, 60 dB, 30 s, intermittent) and novel sound (500 Hz, 60 dB, 30 s, consecutive) were used as the auditory CS+ and CS−. Animals were intraperitoneally injected with KA (20 mg/kg) to induce CIS. Throughout the training session, animals were exposed to a CS for CIS-pairing group, while the control group received CIS or CS alone. After 1.5 hours of pairing training, the training session was stopped, and the mice were given SP to terminate CIS and returned to the home cage.

Testing

Two weeks later, in the test session, the mice were exposed to the CS+ for 15 min to test whether epileptic seizures could be induced by the CS+ or CS−. Additional test sessions could be added as needed, following the same conditions as described.

CSM paradigm within an electrical kindling framework

The stereotaxic surgery followed the same procedure as the microwire electrode arrays for EEG recording. For implantation of stimulating electrodes, coordinates of regions of interest were determined according to the atlas of mice brain coordinates as follows: left hippocampal CA3 (A/P, −2.9 mm; M/L, −3.0 mm; D/V, −3.2 mm). The hand-made electrode was made of Teflon-coated stainless steel wire (791500, DA 0.127 mm, A.M. System, USA), which was twisted into a double-stranded spiral at a certain density (*81*). The double-stranded spiral electrode was split into a u-shape and peel off 0.5 mm of insulation at the tip of the electrode with a surgical blade to allow for electrical stimulation. For scalp EEG recording, silver wire wrapped around the anterior bregma screw and posterior lambda screw for cortical EEG recording and grounding reference, respectively.

After 1 week of surgery recovery, stimulations were administrated by a constant current stimulator (SEN-7203, SS-202 J, Nihon Kohden, Japan) through a bipolar electrode in the left ventral hippocampal CA3, and the scalp EEGs were recorded with a digital amplifier. All mice received ten kindling stimulations daily (400 μA, 20 Hz, 2-s trains, 1-ms monophasic square-wave pulses, 30 min apart, 10 times) for 3 days. The severity of behavioral seizures was scored according to Racine scale (*56*): (i) immobility followed by facial clonus, (ii) masticatory movements and head nodding, (iii) continuous body tremor or wet-dog shakes, (iv) unilateral or bilateral forelimb clonus, and (v) rearing and falling. Stages i to iii are considered focal seizures, and stages iv and v are generalized seizures (*82*). When mice exhibited three consecutive stage v seizures, they were regarded as fully kindled. The seizure stage was scored by an investigator blinded to the group allocation.

In the training session, the kindling-induced seizure was used as the US, and olfactory cues were used as the CS. Lemon odor was used as the olfactory cues. Throughout the training session, animals were exposed to lemon odor for kindling + odor pairing group, while the kindling alone group received kindling stimulations alone. After 3 days of pairing training, the training session was stopped. The next day, in the test session, the mice were exposed to lemon odor to test whether seizures could be induced by the kindling-paired cue. Additional test sessions could be added as needed, following the same conditions as described.

Tissue sample preparation and Western blotting

The procedures were based on our previous study (*83*). After decapitation, the brains were rapidly extracted and frozen in −60°C *N*-hexane. The brains were then transferred to a −80°C freezer. Bilateral tissue punches (16 gauge) of the hippocampus were placed in 1.5-ml microtubes that contained ice-cold radioimmunoprecipitation assay lysis buffer (Applygen Technologies, Beijing, China). After homogenization by an electrical disperser (Wiggenhauser, Sdn Bhd), the homogenate was centrifuged at 12,000 rpm for 10 min at 4°C. All of the above procedures were performed under low temperatures (0° to 4°C). The protein concentrations of the samples were determined using the bicinchoninic acid assay (Applygen Technologies, Beijing, China). The samples were further diluted in radioimmunoprecipitation assay lysis buffer to equalize the protein concentrations. Loading buffer (5×) (16% glycerol, 20% β-mercaptoethanol, 2% SDS, and 0.05% bromophenol blue) was added to each sample (4:1, sample: loading buffer) before being boiled for 5 min. Proteins were separated by 10 to 15% SDS–polyacrylamide gel electrophoresis, transferred to polyvinylidene difluoride membranes (Millipore), and blocked for 1 hour in 5% bovine serum albumin in tris-buffered saline plus 0.05% Tween 20 (pH 7.4). Primary antibodies [anti-BDNF, 1:3000; anti-EGR1, 1:1000; anti-pmTOR (Ser^{2448}), 1:1000; anti-mTOR, 1:1000; anti–β-actin, 1:5000; anti–ERK1 + ERK2, 1:2000; anti–Erk1

(pT202/pY204) + Erk2 (pT185/pY187), 1:1000] and horseradish peroxidase–conjugated secondary antibodies (goat anti-rabbit immunoglobulin G, 1:2000; goat anti-mouse immunoglobulin G, 1:5000) were used. The band intensities were quantified by two observers who were blind to the experimental groups using Quantity One 4.4.0 software (Bio-Rad, Hercules, CA, USA).

Human clinical trial

The double-blind, randomized, placebo-controlled study (NCT05613166) to evaluate the efficacy of everolimus on refractory epilepsy was approved by the Ethics Committee of Shengjing Hospital of China Medical University. Participants were recruited and signed an informed consent form. Key inclusion criteria were (i) over 18 years of age, (ii) clinically diagnosed as refractory epilepsy, (iii) seizures that can be clearly identified by EEG, and (iv) no drug interaction between the original AEDs and everolimus, and the AEDs had been taken for at least 12 weeks before enrollment. Key exclusion criteria were (i) patients who were or had been treated with mTOR inhibitors, (ii) seizures secondary to drug abuse, (iii) patients who had a persistent epileptic state within 1 year before enrollment, and (iv) patients with ≥ 2 seizures per 24 hours.

Eligible patients enrolled in this study were randomly assigned into 3 groups at a 1:1:1 ratio: 1-hour treatment group, 8-hour delayed administration treatment group, and the negative control group. They orally received a single dose of everolimus or placebo (vitamin C) 1 or 8 hours after an epileptic seizure event, while continuing their previous AEDs throughout the study. On the basis of the subject's body surface area (BSA), the dosage of everolimus was adjusted to either 5 mg per dose (for BSA, 1.3 to 2.1 m^2) or 7.5 mg per dose (for BSA, $\geq$2.2 m^2). Scalp EEG (64 channels; Nicolet, USA) with a 10 to 20 system was used for monitoring through the predrug period (baseline) to the postdrug period for each patient. Predrug period and postdrug period included at least wakefulness and sleep periods to mark background rhythm and IED rhythm. The frequency of IEDs after drug administration compared to baseline was evaluated as the primary end point.

Statistical analysis

For in vivo experiments, the animals were distributed into various treatment groups randomly. Statistical analyses were performed using GraphPad Prism 9 (GraphPad Software) and SPSS 26.0 software (SPSS Inc.). Before statistical analysis, variation within each group of data and the assumptions of the tests were checked. Comparisons between two groups were made using Student's paired or unpaired two-tailed *t* tests and two-tailed Welch's *t* tests or nonparametric (Wilcoxon rank sum) tests as appropriate. Comparisons among three or more groups were made using one-way analysis of variance (ANOVA) analyses, followed by Bonferroni's multiple-comparisons test. No statistical methods were used to predetermine sample sizes, but our sample sizes are similar to those reported previously in the field (*84*, *85*). All experiments and analyses of data were performed in a blinded manner by investigators who were unaware of the genotype or manipulation. All data in the article are presented in the form of mean ± SD. Any exceptions to this format are explicitly stated in the figure legends. Statistical significance of differences at $P < 0.05$ was indicated as an asterisk (*), $P < 0.01$ was indicated as two asterisks (**), and $P < 0.001$ was shown with three asterisks (***) in all figures. Detailed statistical information is provided in table S1.

Supplementary Materials

This PDF file includes:
Figs. S1 to S6
Legend for table S1

Other Supplementary Material for this manuscript includes the following:
Table S1

REFERENCES AND NOTES

1. K. J. Meador, The basic science of memory as it applies to epilepsy. *Epilepsia* **48**, 23–25 (2007).
2. R. Das, A. Luczak, Epileptic seizures and link to memory processes. *AIMS Neurosci* **9**, 114–127 (2022).
3. G. V. Goddard, R. M. Douglas, Does the engram of kindling model the engram of normal long term memory? *Can. J. Neurol. Sci.* **2**, 385–394 (1975).
4. D. Hsu, W. Chen, M. Hsu, J. M. Beggs, An open hypothesis: Is epilepsy learned, and can it be unlearned? *Epilepsy Behav.* **13**, 511–522 (2008).
5. R. S. Fisher, C. Acevedo, A. Arzimanoglou, A. Bogacz, J. H. Cross, C. E. Elger, J. Engel Jr., L. Forsgren, J. A. French, M. Glynn, D. C. Hesdorffer, B. I. Lee, G. W. Mathern, S. L. Moshe, E. Perucca, I. E. Scheffer, T. Tomson, M. Watanabe, S. Wiebe, ILAE official report: A practical clinical definition of epilepsy. *Epilepsia* **55**, 475–482 (2014).
6. Z. V. Okudan, Ç. Özkara, Reflex epilepsy: Triggers and management strategies. *Neuropsychiatr. Dis. Treat.* **14**, 327–337 (2018).
7. D. Italiano, E. Ferlazzo, S. Gasparini, E. Spina, S. Mondello, A. Labate, A. Gambardella, U. Aguglia, Generalized versus partial reflex seizures: A review. *Seizure* **23**, 512–520 (2014).
8. A. Dickinson, Conditioning and associative learning. *Br. Med. Bull.* **37**, 165–168 (1981).
9. H. E. Scharfman, Epilepsy as an example of neural plasticity. *Neuroscientist* **8**, 154–173 (2002).
10. M. Lynch, U. Sayin, G. Golarai, T. Sutula, NMDA receptor-dependent plasticity of granule cell spiking in the dentate gyrus of normal and epileptic rats. *J. Neurophysiol.* **84**, 2868–2879 (2000).
11. Y. Ruan, C. Xu, J. Lan, J. Nao, S. Zhang, F. Fan, Y. Wang, Z. Chen, Low-frequency stimulation at the subiculum is anti-convulsant and anti-drug-resistant in a mouse model of lamotrigine-resistant temporal lobe epilepsy. *Neurosci. Bull.* **36**, 654–658 (2020).
12. I. Mody, U. Heinemann, NMDA receptors of dentate gyrus granule cells participate in synaptic transmission following kindling. *Nature* **326**, 701–704 (1987).
13. E. Paschen, C. Elgueta, K. Heining, D. M. Vieira, P. Kleis, C. Orcinha, U. Häussler, M. Bartos, U. Egert, P. Janz, C. A. Haas, Hippocampal low-frequency stimulation prevents seizure generation in a mouse model of mesial temporal lobe epilepsy. *eLife* **9**, e54518 (2020).
14. G. V. Goddard, D. C. McIntyre, C. K. Leech, A permanent change in brain function resulting from daily electrical stimulation. *Exp. Neurol.* **25**, 295–330 (1969).
15. M. R. Bower, M. T. Kucewicz, E. K. St Louis, F. B. Meyer, W. R. Marsh, M. Stead, G. A. Worrell, Reactivation of seizure-related changes to interictal spike shape and synchrony during postseizure sleep in patients. *Epilepsia* **58**, 94–104 (2017).
16. M. R. Bower, M. Stead, R. S. Bower, M. T. Kucewicz, V. Sulc, J. Cimbalnik, B. H. Brinkmann, V. M. Vasoli, E. K. St Louis, F. B. Meyer, W. R. Marsh, G. A. Worrell, Evidence for consolidation of neuronal assemblies after seizures in humans. *J. Neurosci.* **35**, 999–1010 (2015).
17. I. P. Pavlov, *Conditioned Reflexes* (Oxford Univ. Press, 1927).
18. R. W. Semon, *The Mneme* (G. Allen & Unwin Limited, 1921).
19. D. O. Hebb, *The Organization of Behavior: A Neuropsychological Theory* (Science Education, John Wiley and Sons Inc., 1949).
20. S. Tonegawa, X. Liu, S. Ramirez, R. Redondo, Memory engram cells have come of age. *Neuron* **87**, 918–931 (2015).
21. S. A. Josselyn, S. Köhler, P. W. Frankland, Finding the engram. *Nat. Rev. Neurosci.* **16**, 521–534 (2015).
22. K. Nader, G. E. Schafe, J. E. Le Doux, Fear memories require protein synthesis in the amygdala for reconsolidation after retrieval. *Nature* **406**, 722–726 (2000).
23. N. C. Tronson, J. R. Taylor, Molecular mechanisms of memory reconsolidation. *Nat. Rev. Neurosci.* **8**, 262–275 (2007).
24. K. Nader, Reconsolidation and the dynamic nature of memory. *Cold Spring Harb. Perspect. Biol.* **7**, a021782 (2015).
25. J. L. C. Lee, K. Nader, D. Schiller, An update on memory reconsolidation updating. *Trends Cogn. Sci.* **21**, 531–545 (2017).
26. C. M. Alberini, The role of reconsolidation and the dynamic process of long-term memory formation and storage. *Front. Behav. Neurosci.* **5**, 12 (2011).
27. L. Schwabe, K. Nader, J. C. Pruessner, Reconsolidation of human memory: Brain mechanisms and clinical relevance. *Biol. Psychiatry* **76**, 274–280 (2014).
28. S. S. Pattwell, K. G. Bath, B. J. Casey, I. Ninan, F. S. Lee, Selective early-acquired fear memories undergo temporary suppression during adolescence. *Proc. Natl. Acad. Sci. U.S.A.* **108**, 1182–1187 (2011).

29. R. J. Racine, Modification of seizure activity by electrical stimulation: II. Motor seizure. *Electroencephalogr Clin Neurophysiol* **32**, 281–294 (1972).
30. P. A. Williams, A. M. White, S. Clark, D. J. Ferraro, W. Swiercz, K. J. Staley, F. E. Dudek, Development of spontaneous recurrent seizures after kainate-induced status epilepticus. *J. Neurosci.* **29**, 2103–2112 (2009).
31. Y. Ben-Ari, R. Cossart, Kainate, a double agent that generates seizures: Two decades of progress. *Trends Neurosci.* **23**, 580–587 (2000).
32. H. S. White, Animal models of epileptogenesis. *Neurology* **59**, S7–S14 (2002).
33. S. Ramirez, X. Liu, P.-A. Lin, J. Suh, M. Pignatelli, R. L. Redondo, T. J. Ryan, S. Tonegawa, Creating a false memory in the hippocampus. *Science* **341**, 387–391 (2013).
34. G. Vetere, L. M. Tran, S. Moberg, P. E. Steadman, L. Restivo, F. G. Morrison, K. J. Ressler, S. A. Josselyn, P. W. Frankland, Memory formation in the absence of experience. *Nat. Neurosci.* **22**, 933–940 (2019).
35. F. de Castro, Wiring olfaction: The cellular and molecular mechanisms that guide the development of synaptic connections from the nose to the cortex. *Front. Neurosci.* **3**, 52 (2009).
36. T. Hainmueller, M. Bartos, Dentate gyrus circuits for encoding, retrieval and discrimination of episodic memories. *Nat. Rev. Neurosci.* **21**, 153–168 (2020).
37. N. I. Woods, F. Stefanini, D. L. Apodaca-Montano, I. M. C. Tan, J. S. Biane, M. A. Kheirbek, The dentate gyrus classifies cortical representations of learned stimuli. *Neuron* **107**, 173–184.e6 (2020).
38. C. J. Guenthner, K. Miyamichi, H. H. Yang, H. C. Heller, L. Luo, Permanent genetic access to transiently active neurons via TRAP: Targeted recombination in active populations. *Neuron* **78**, 773–784 (2013).
39. T. Kawashima, K. Kitamura, K. Suzuki, M. Nonaka, S. Kamijo, S. Takemoto-Kimura, M. Kano, H. Okuno, K. Ohki, H. Bito, Functional labeling of neurons and their projections using the synthetic activity-dependent promoter E-SARE. *Nat. Methods* **10**, 889–895 (2013).
40. J. Debiec, J. E. LeDoux, K. Nader, Cellular and systems reconsolidation in the hippocampus. *Neuron* **36**, 527–538 (2002).
41. L. Bellfy, J. L. Kwapis, Molecular mechanisms of reconsolidation-dependent memory updating. *Int. J. Mol. Sci.* **21**, 6580 (2020).
42. M. C. Gonzalez, A. Radiske, M. Cammarota, On the involvement of BDNF signaling in memory reconsolidation. *Front. Cell. Neurosci.* **13**, 383 (2019).
43. M. C. Gonzalez, J. I. Rossato, A. Radiske, M. Pádua Reis, M. Cammarota, Recognition memory reconsolidation requires hippocampal Zif268. *Sci. Rep.* **9**, 16620 (2019).
44. C. A. Hoeffer, E. Klann, mTOR signaling: At the crossroads of plasticity, memory and disease. *Trends Neurosci.* **33**, 67–75 (2010).
45. G. M. Gafford, R. G. Parsons, F. J. Helmstetter, Consolidation and reconsolidation of contextual fear memory requires mammalian target of rapamycin-dependent translation in the dorsal hippocampus. *Neuroscience* **182**, 98–104 (2011).
46. C. M. Atkins, J. C. Selcher, J. J. Petraitis, J. M. Trzaskos, J. D. Sweatt, The MAPK cascade is required for mammalian associative learning. *Nat. Neurosci.* **1**, 602–609 (1998).
47. Á. Kelly, S. Laroche, S. Davis, Activation of mitogen-activated protein kinase/extracellular signal-regulated kinase in hippocampal circuitry is required for consolidation and reconsolidation of recognition memory. *J. Neurosci.* **23**, 5354–5360 (2003).
48. X. Ye, D. Kapeller-Libermann, A. Travaglia, M. C. Inda, C. M. Alberini, Direct dorsal hippocampal-prelimbic cortex connections strengthen fear memories. *Nat. Neurosci.* **20**, 52–61 (2017).
49. J. Bockaert, P. Marin, mTOR in brain physiology and pathologies. *Physiol. Rev.* **95**, 1157–1187 (2015).
50. N. V. Kukushkin, T. Tabassum, T. J. Carew, Precise timing of ERK phosphorylation/dephosphorylation determines the outcome of trial repetition during long-term memory formation. *Proc. Natl. Acad. Sci. U.S.A.* **119**, e2210478119 (2022).
51. T. Agren, J. Engman, A. Frick, J. Björkstrand, E.-M. Larsson, T. Furmark, M. Fredrikson, Disruption of reconsolidation erases a fear memory trace in the human amygdala. *Science* **337**, 1550–1552 (2012).
52. D. Schiller, M.-H. Monfils, C. M. Raio, D. C. Johnson, J. E. Ledoux, E. A. Phelps, Preventing the return of fear in humans using reconsolidation update mechanisms. *Nature* **463**, 49–53 (2010).
53. A. Brunet, S. P. Orr, J. Tremblay, K. Robertson, K. Nader, R. K. Pitman, Effect of post-retrieval propranolol on psychophysiologic responding during subsequent script-driven traumatic imagery in post-traumatic stress disorder. *J. Psychiatr. Res.* **42**, 503–506 (2008).
54. Y.-X. Xue, J.-H. Deng, Y.-Y. Chen, L.-B. Zhang, P. Wu, G.-D. Huang, Y.-X. Luo, Y.-P. Bao, Y.-M. Wang, Y. Shaham, J. Shi, L. Lu, Effect of selective inhibition of reactivated nicotine-associated memories with propranolol on nicotine craving. *JAMA Psychiatry* **74**, 224–232 (2017).
55. S. Barak, F. Liu, S. Ben Hamida, Q. V. Yowell, J. Neasta, V. Kharazia, P. H. Janak, D. Ron, Disruption of alcohol-related memories by mTORC1 inhibition prevents relapse. *Nat. Neurosci.* **16**, 1111–1117 (2013).
56. X. Liu, L. Ma, H. H. Li, B. Huang, Y. X. Li, Y. Z. Tao, L. Ma, β-Arrestin-biased signaling mediates memory reconsolidation. *Proc. Natl. Acad. Sci. U.S.A.* **112**, 4483–4488 (2015).
57. M. Guida, A. Iudice, E. Bonanni, F. S. Giorgi, Effects of antiepileptic drugs on interictal epileptiform discharges in focal epilepsies: An update on current evidence. *Expert Rev. Neurother.* **15**, 947–959 (2015).
58. C.-C. Lee, C.-C. Chou, F.-J. Hsiao, Y.-H. Chen, C.-F. Lin, C.-J. Chen, S.-J. Peng, H.-L. Liu, H.-Y. Yu, Pilot study of focused ultrasound for drug-resistant epilepsy. *Epilepsia* **63**, 162–175 (2022).
59. R. J. Joynt, D. Green, R. Green, Musicogenic epilepsy. *JAMA* **179**, 501–504 (1962).
60. G. Harding, A. J. Wilkins, G. Erba, G. L. Barkley, R. S. Fisher, Epilepsy Foundation of America Working Group, Photic- and pattern-induced seizures: Expert consensus of the Epilepsy Foundation of America Working Group. *Epilepsia* **46**, 1423–1425 (2005).
61. F. Ilik, A. C. Pazarli, Reflex epilepsy triggered by smell. *Clin. EEG Neurosci.* **46**, 263–265 (2015).
62. N. Nevler, R. Gandelman-Marton, Acute provoked reflex seizures induced by thinking. *Neurologist* **18**, 415–417 (2012).
63. J. Isnard, M. Guénot, C. Fischer, P. Mertens, M. Sindou, F. Mauguière, A stereoelectroencephalographic (SEEG) study of light-induced mesiotemporal epileptic seizures. *Epilepsia* **39**, 1098–1103 (1998).
64. C. Vollmar, J. O'Muircheartaigh, G. J. Barker, M. R. Symms, P. Thompson, V. Kumari, J. S. Duncan, D. Janz, M. P. Richardson, M. J. Koepp, Motor system hyperconnectivity in juvenile myoclonic epilepsy: A cognitive functional magnetic resonance imaging study. *Brain* **134**, 1710–1719 (2011).
65. G. Varotto, E. Visani, L. Canafoglia, S. Franceschetti, G. Avanzini, F. Panzica, Enhanced frontocentral EEG connectivity in photosensitive generalized epilepsies: A partial directed coherence study. *Epilepsia* **53**, 359–367 (2012).
66. E. R. Kandel, J. H. Schwartz, T. M. Jessell, S. Siegelbaum, A. J. Hudspeth, S. Mack, *Principles of neural science* (McGraw Hill, 2000), vol. 4.
67. Y. Geinisman, F. Morrell, L. deToledo-Morrell, Remodeling of synaptic architecture during hippocampal "kindling". *Proc. Natl. Acad. Sci. U.S.A.* **85**, 3260–3264 (1988).
68. R. J. Racine, N. W. Milgram, S. Hafner, Long-term potentiation phenomena in the rat limbic forebrain. *Brain Res.* **260**, 217–231 (1983).
69. R. P. Bonin, Y. De Koninck, A spinal analog of memory reconsolidation enables reversal of hyperalgesia. *Nat. Neurosci.* **17**, 1043–1045 (2014).
70. P. Kwan, M. J. Brodie, Early identification of refractory epilepsy. *N. Engl. J. Med.* **342**, 314–319 (2000).
71. R. Mohanraj, M. J. Brodie, Diagnosing refractory epilepsy: Response to sequential treatment schedules. *Eur. J. Neurol.* **13**, 277–282 (2006).
72. R. D. Thijs, R. Surges, T. J. O'Brien, J. W. Sander, Epilepsy in adults. *Lancet* **393**, 689–701 (2019).
73. Y. Wang, Z. Chen, An update for epilepsy research and antiepileptic drug development: Toward precise circuit therapy. *Pharmacol. Ther.* **201**, 77–93 (2019).
74. Y. Liu, S. Lai, W. Ma, W. Ke, C. Zhang, S. Liu, Y. Zhang, F. Pei, S. Li, M. Yi, Y. Shu, Y. Shang, J. Liang, Z. Huang, CDYL suppresses epileptogenesis in mice through repression of axonal Nav1.6 sodium channel expression. *Nat. Commun.* **8**, 355 (2017).
75. J. F. Flood, M. R. Rosenzweig, E. L. Bennett, A. E. Orme, The influence of duration of protein synthesis inhibition on memory. *Physiol. Behav.* **10**, 555–562 (1973).
76. J. L. Lee, B. J. Everitt, K. L. Thomas, Independent cellular processes for hippocampal memory consolidation and reconsolidation. *Science* **304**, 839–843 (2004).
77. M. M. Shah, A. E. Anderson, V. Leung, X. Lin, D. Johnston, Seizure-induced plasticity of h channels in entorhinal cortical layer III pyramidal neurons. *Neuron* **44**, 495–508 (2004).
78. X.-P. He, R. Kotloski, S. Nef, B. W. Luikart, L. F. Parada, J. O. McNamara, Conditional deletion of TrkB but not BDNF prevents epileptogenesis in the kindling model. *Neuron* **43**, 31–42 (2004).
79. Z. Huang, M. C. Walker, M. M. Shah, Loss of dendritic HCN1 subunits enhances cortical excitability and epileptogenesis. *J. Neurosci.* **29**, 10979–10988 (2009).
80. M. Lévesque, M. Avoli, The kainic acid model of temporal lobe epilepsy. *Neurosci. Biobehav. Rev.* **37**, 2887–2899 (2013).
81. N. Lai, Z. Li, Z. Chen, Y. Wang, Protocol for labeling epileptic-status-related neuronal ensembles in mouse hippocampal kindling model. *STAR Protoc* **4**, 102255 (2023).
82. M. Sato, R. J. Racine, D. C. McIntyre, Kindling: Basic mechanisms and clinical validity. *Electroencephalogr. Clin. Neurophysiol.* **76**, 459–472 (1990).
83. Y.-X. Xue, L.-F. Xue, J.-F. Liu, J. He, J.-H. Deng, S.-C. Sun, H.-B. Han, Y.-X. Luo, L.-Z. Xu, P. Wu, L. Lu, Depletion of perineuronal nets in the amygdala to enhance the erasure of drug memories. *J. Neurosci.* **34**, 6647–6658 (2014).
84. Z. Huang, R. Lujan, I. Kadurin, V. N. Uebele, J. J. Renger, A. C. Dolphin, M. M. Shah, Presynaptic HCN1 channels regulate Cav3.2 activity and neurotransmission at select cortical synapses. *Nat. Neurosci.* **14**, 478–486 (2011).
85. Z. Huang, R. Lujan, J. Martinez-Hernandez, A. S. Lewis, D. M. Chetkovich, M. M. Shah, TRIP8b-independent trafficking and plasticity of adult cortical presynaptic HCN1 channels. *J. Neurosci.* **32**, 14835–14848 (2012).

Acknowledgments: We thank L.-Z. Guan from Beijing Normal University for help with EEG recording. We thank Y. Wang from Zhejiang University for help with kindling model. **Funding:** This work was supported by STI2030-Major Projects (2021ZD0202103 to Z.H.); National Natural Science Foundation of China (82271498 to Z.H.); Ningxia Hui Autonomous Region Key Research and Development Project (2022BEG02042 to Z.H.); Science Foundation of Peking University Cancer Hospital (JC202304 to Z.H.); National Natural Science Foundation of China (82071498 to Y.-X.X.); National Natural Science Foundation of China (32161143022 to Y.-X.X.); STI2030-Major Projects (2022ZD0214500 to Y.-X.X.); Scientific Project of Beijing Life Science Academy (2023300CB0100 to Y.-X.X.); Research Grants Council, University Grants Committee, Hong Kong (11104320 to C.G.L.); Research Grants Council, University Grants Committee, Hong Kong (11104521 to C.G.L.); Natural Science Foundation of Sichuan Province (grant no. 2023NSFSC1572 to S.La.); and The Project for Excellent Talents in Xihua University (grant no. Z211062 to S.La.). **Author contributions:** Conceptualization: Z.H. and Y.-X.X. Methodology: S.La., L.Z., X.T., X.M., Y.S., K.C., M.L., J.M., W.M., C.Y., Y.S., Q.W., and Z.L. Investigation: Z.H., Y.-X.X., S. Li, and J.S. Visualization: S.La., L.Z., X.T., and X.M. Supervision: Z.H., Y.-X.X., S. Li, J.S., and W.M. Writing—original draft: Z.H., Y.-X.X., S.La., L.Z., X.T., W.M., and X.M. Writing—review and editing: Z.H., C.G.L., Y.-X.X., S.La., L.Z., X.T., and X.M. **Competing interests:** The authors declare that they have no competing interests. **Data and materials availability:** All data needed to evaluate the conclusions in the paper are present in the paper and/or the Supplementary Materials.

Submitted 19 September 2023
Accepted 13 February 2024
Published 20 March 2024
10.1126/sciadv.adk9484